Electroluminescence imaging and microstructure of organic light-emitting field-effect transistors

Jana Zaumseil,[1] R. Joseph Kline,[2] and Henning Sirringhaus[1,a)]
[1]*Cavendish Laboratory, Department of Physics, University of Cambridge, J.J. Thomson Av., Cambridge CB3 0HE, United Kingdom*
[2]*Polymers Division, National Institute of Standards and Technology, 100 Bureau Dr., Gaithersburg, Maryland 20899, USA*

(Received 15 October 2007; accepted 19 December 2007; published online 20 February 2008)

The effect of morphology and microstructure on the emission characteristics of ambipolar light-emitting field-effect transistors is studied using the polyfluorene copolymer F8BT [poly(9,9-di-*n*-octylfluorene-*alt*-benzothiadiazole)] as a model system. Different intensity distributions of the emission zones of amorphous, polycrystalline, and aligned F8BT films are demonstrated. Electroluminescence maps of the channel region are produced by overlaying a series of images recorded during gate voltage sweeps. They show a correlation to the microcrystalline structure of the F8BT and are assumed to visualize the current density distribution within the transistor channel. © *2008 American Institute of Physics*. [DOI: 10.1063/1.2836790]

Micro- and nanostructure of organic semiconductors are highly important for their charge transport, luminescence, and charge separation characteristics. This is especially true for devices such as light-emitting diodes,[1,2] photovoltaic cells,[3,4] and field-effect transistors[5,6] (FETs) that rely on blends of different semiconducting materials. However, even in devices with a single semiconducting component, inhomogeneities in electronic structure can arise due to variations in intermolecular packing, molecular conformation, or orientation. Crystallization in semicrystalline polymers leads to chain orientation variations on mesoscopic lengthscales and grain boundaries with amorphous interstices. Such spatial differences in microstructure are expected to affect local charge carrier mobility and current density,[7,8] exciton formation, diffusion, and quenching.[9,10] Various optical and scanning microscopy techniques have been used to elucidate the relationship between microstructure and optoelectronic properties with the objective to improve device performance.[4,11–14] In the case of organic FETs, scanning Kelvin probe and electric force microscopy were used to image the local potential and thus the electric field distribution within the channel but not the lateral current flow.[11,12] On the contrary, they must assume a constant current density, which is unlikely in a semiconductor film with regions of high and low mobilities. Here, we show that mapping of current paths could instead be achieved by using electroluminescence (EL) from light-emitting FETs as a measure of the local current density.

Organic light-emitting field-effect transistors (LFETs) are bifunctional devices combining gate control and high lateral charge carrier mobilities with light emission.[15] In an ambipolar LFET, positive and negative charge carriers can accumulate in spatially separate regions under suitable biasing conditions. Due to their planar structure, they allow observation and spatial resolution of a narrow recombination and emission zone where the hole and electron accumulation layers meet. This zone can be moved through the entire channel by changing the applied gate (V_g) or source-drain voltage (V_{ds}).[16–18] We use this feature of ambipolar LFETs to investigate charge transport paths in polymer semiconductors with different amorphous, polycrystalline, and aligned nematic microstructures. As model systems, we used bottom contact/top gate ambipolar F8BT-LFETs with a poly(methyl methacrylate) (PMMA) gate dielectric. The semiconductor F8BT is a green-emitting polyfluorene whose optoelectronic and structural properties are well established.[19,20]

The schematic device structure is shown in the inset of Fig. 1(a). FETs with interdigitated electrodes were fabricated as described previously.[18] F8BT (M_n=62 kg mol^{-1}) films of about 160 nm thickness were annealed at 290 °C for 30 min and slowly cooled to induce polycrystallinity with large crystallites.[19] F8BT films annealed at 120 °C (below glass transition temperature) remained amorphous without any microstructural features resolved by optical microscopy. For FETs with aligned F8BT, a polyimide layer (PI2525, HD Microsystems) (Ref. 21) was spincoated onto the glass substrate, cured in nitrogen, and mechanically rubbed before source/drain gold electrodes were evaporated. Annealing of the subsequently spincoated F8BT layer to the liquid crystalline melt and quenching resulted in a nematic glass with polymer chains predominantly aligned along the rubbing direction.

F8BT-FETs showed reproducible, ambipolar current-voltage characteristics, as shown in Fig. 1(a), for a transistor with polycrystalline F8BT. An optical image of the emission zone of this LFET is shown in Fig. 1(b). In comparison, Fig. 1(c) shows the emission zone of a LFET with an amorphous F8BT layer.[22] While light emission from the amorphous F8BT film is quite narrow (width at half maximum of ≈2 μm) and featureless, the emission zone of the polycrystalline polymer film is much broader (≈4 μm) and shows bright spots of various shapes and sizes and dark gaps. Although the intensity distribution in Fig. 1(b) immediately appears to be related to the polycrystalline morphology of the F8BT film, it is unclear whether this is due to variations of photoluminescence (PL) efficiency, outcoupling efficiency, current density or variations in nonradiative recombination due to trap sites.

We can generate a map of electroluminescence of the whole channel region by overlaying all images recorded during a gate voltage sweep at constant V_{ds}. During such a scan,

a)Electronic mail: hs220@cam.ac.uk.

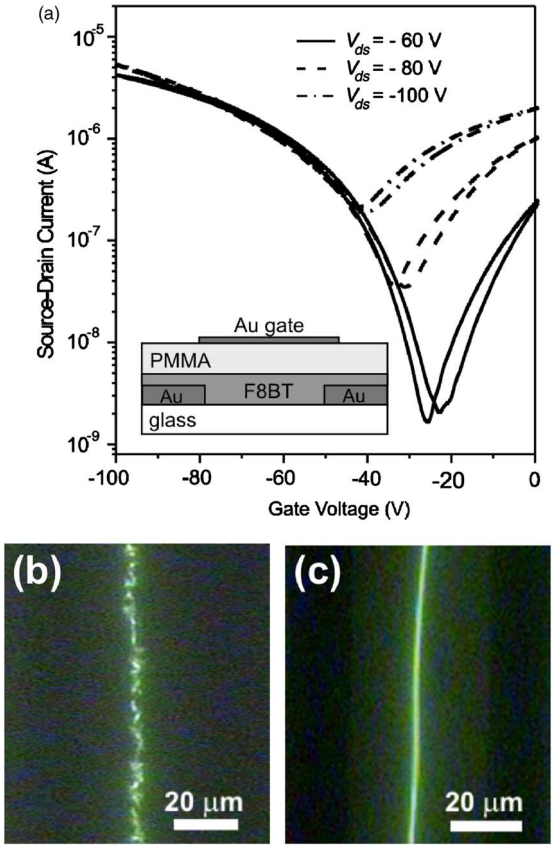

FIG. 1. (Color online) (a) Transfer characteristics (forward and reverse) of a LFET with bottom contact gold electrodes (L=40 μm, W/L=500), polycrystalline F8BT (160 nm), PMMA (Polymer Source, Inc.) gate dielectric (400 nm, C_i=8 nF cm^{-2}), and gold top gate electrode (inset: schematic structure). Saturation hole and electron mobilities were 5×10^{-4} and 2.5×10^{-4} cm^2 V^1 s^{-1}, respectively. Optical image of emission zone of (b) polycrystalline and of (c) amorphous F8BT-LFETs.

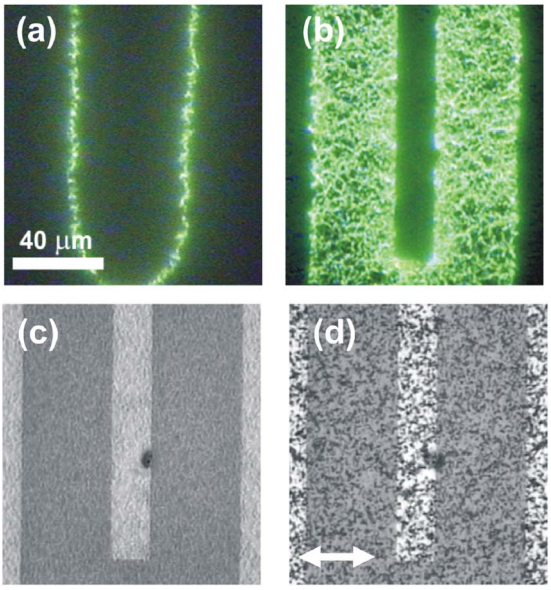

FIG. 2. (Color online) (a) Optical image of emission zone in polycrystalline F8BT-LFET with interdigitated source/drain electrodes. (b) EL map produced by overlaying a series of images during a V_g sweep. Note that I_{sd} changes during a V_g sweep, leading to slightly higher intensities toward the electrode edges. PL images of the same region (same length scale) as in (a) and (b): (c) without polarizer and (d) with polarizer parallel to charge transport direction.

the emission zone moves from the drain to the source electrode and vice versa. This method, illustrated in Fig. 2, allows us to compare the EL image with a PL image of the same area. A single image of the emission zone of a polycrystalline F8BT-LFET with interdigitated electrodes is shown in Fig. 2(a), while Fig. 2(b) shows an EL map after overlaying more than 100 single images recorded at different V_g (scanned at 2 V s^{-1}). The overall image is calculated by assigning to each pixel a color corresponding to the highest brightness value this pixel exhibited during the entire voltage sweep. This EL map shows that certain areas of the channel region never light up and remain dark for all voltage conditions, while the bright regions of the channel form a type of fractal network. The bright areas are isotropic (see Fourier transformation of the EL map in Fig. S1(a) in Ref. 22), and the brightness histogram shows one broad distribution and a second narrow distribution at higher brightnesses, indicating strongly preferred areas of emission (Fig. S1(b) in Ref. 22).

The correlation of this EL map with a simple fluorescence image [Fig. 2(c)], which reflects the distribution of PL and outcoupling efficiency of the polycrystalline film, is poor. The PL image shows little intensity variations and the brighter regions do not coincide with bright features of the EL map. Previous studies also showed that the PL efficiency of F8BT varies only between 45% and 55% with molecular weight and morphology.[19] We can therefore exclude differences of PL or outcoupling efficiency to be the origin of the emission distribution in polycrystalline F8BT-LFETs. We can also rule out extended, long lived charge trapping and quenching sites to be the origin of dark areas because the EL maps for forward and reverse voltage sweeps, i.e., from electron to hole accumulation and vice versa, are identical and do not show any hysteretic features (see Fig. S1(c)–S1(e) in Ref. 22).

This strongly suggests that lateral variations in current density are responsible for the observed variations in emitted light intensity. Since the amount of emitted light increases with the number of charge carriers recombining in a certain area, the bright areas should correspond to F8BT regions with higher current density. Note, for example, that the surroundings of the tip of the drain electrode [bottom center in Fig. 2(b)] are much brighter than the adjacent areas. The asymmetric electrode geometry leads to a concentration of electric field and current in this area and hence brighter emission. Current density variations can also arise from areas of high and low mobilities. In an amorphous polymer, the carrier mobility is isotropic and should hence lead to a uniform current density and a featureless emission zone, as seen in Fig. 1(c). However, polyfluorenes that were thermally treated into the nematic liquid crystalline phase are known to exhibit highly anisotropic carrier mobilities. When the polymer chains are aligned parallel to the transport direction, the field-effect mobility is found to be up to ten times higher than that for perpendicular orientation with respect to the transport direction.[23,24] In a polycrystalline film with domains of different orientations, charge carriers should be more likely to pass through F8BT regions aligned along the lateral field, circumventing those aligned perpendicular. These high mobility regions should thus exhibit higher current densities and higher EL intensity. The polarized PL image in Fig. 2(d) shows a distribution of dark (bright) regions representing crystallites with polymer chains perpendicular (parallel) to the polarization and charge transport direction. These domains are on a similar length scale as the bright and

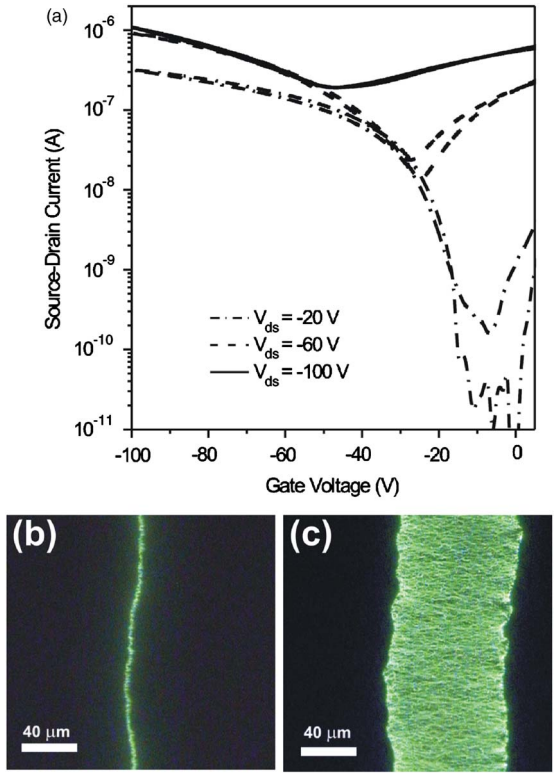

FIG. 3. (Color online) (a) Transfer characteristics (forward and reverse) of LFET with partially aligned F8BT, $L=95\ \mu m$, $W/L=32$, and $C_i=6.4\ nF\ cm^{-2}$. Saturation hole and electron mobilities were 1.5×10^{-3} and $4.3\times10^{-4}\ cm^2\ V^{-1}\ s^{-1}$, respectively. (b) Optical image of emission zone and (c) accumulative EL image of this LFET.

dark features in Fig. 2(b). Similarly, F8BT-LFETs with a finer polycrystalline structure show a much denser EL map (see Fig. S2 in Ref. 22).

However, the EL intensity is not proportionally linked to the carrier mobility but instead reflects in a complex manner the lateral variations in mobility, polymer orientation, and electric field along the current conduction paths for both holes and electrons between source and drain. It is thus not possible to directly correlate bright areas in Fig. 2(b) with those in Fig. 2(d). For example, high current densities could also occur in small areas, in which the polymer is only reasonably well aligned with the current direction, if the surroundings are even less conducting.

Figure 3 shows that current density and emission pattern are nevertheless directly influenced by polymer chain alignment and thus distribution of high and low mobility areas in LFETs. Here, the F8BT film was thermotropically aligned on a rubbed polyimide layer. Although the majority of the polymer is oriented parallel to the transport direction, under the alignment conditions used here, the polymer does not form a large monodomain but contains small misaligned areas (see Figs. S3(a) and S3(b) in Ref. 22). Even so, hole and electron mobilities are significantly higher than those of a polycrystalline F8BT film [Fig. 3(a)]. Again, the light intensity exhibits variations along the emission zone of this LFET [Fig. 3(b)], and when added up to an EL map [Fig. 3(c)], a strong anisotropy of the bright areas and thus current paths is revealed (orientation distribution shown in Fig. S3(c) in Ref. 22). There are clearly preferred current paths and the conduction appears to be of filamentary nature. The intensity distribution [Fig. S3(d)] is narrower and more even than in the case of polycrystalline F8BT-LFET. Due to the almost complete alignment, charges rarely need to circumvent low mobility areas and thus less bright-dark contrast occurs.

In summary, we have shown that the intensity distribution within the emission zone of LFETs has a clear correlation with the microstructure of the semiconducting polymer. EL maps of polycrystalline and aligned LFETs indicate that higher EL intensities arise from areas of high current density. The demonstrated technique of producing EL maps by scanning the emission zone through the channel could be applied to more complex morphologies, such as semiconductor blends.

[1] N. Corcoran, A. C. Arias, J. S. Kim, J. D. MacKenzie, and R. H. Friend, Appl. Phys. Lett. **82**, 299 (2003).
[2] A. C. Morteani, A. S. Dhoot, J. S. Kim, C. Silva, N. C. Greenham, C. Murphy, E. Moons, S. Cina, J. H. Burroughes, and R. H. Friend, Adv. Mater. (Weinheim, Ger.) **15**, 1708 (2003).
[3] L. H. Nguyen, H. Hoppe, T. Erb, S. Gunes, G. Gobsch, and N. S. Sariciftci, Adv. Funct. Mater. **17**, 1071 (2007).
[4] D. C. Coffey, O. G. Reid, D. B. Rodovsky, G. P. Bartholomew, and D. S. Ginger, Nano Lett. **7**, 738 (2007).
[5] E. J. Meijer, D. M. de Leeuw, S. Setayesh, E. van Veenendaal, B. H. Huisman, P. W. M. Blom, J. C. Hummelen, U. Scherf, and T. M. Klapwijk, Nat. Mater. **2**, 678 (2003).
[6] M. A. Loi, C. Rost-Bietsch, M. Murgia, S. Karg, W. Riess, and M. Muccini, Adv. Funct. Mater. **16**, 41 (2006).
[7] R. J. Kline, M. D. McGehee, E. N. Kadnikova, J. S. Liu, J. M. J. Frechet, and M. F. Toney, Macromolecules **38**, 3312 (2005).
[8] K. C. Dickey, J. E. Anthony, and Y. L. Loo, Adv. Mater. (Weinheim, Ger.) **18**, 1721 (2006).
[9] E. Lunedei, P. Moretti, H. Murgia, M. Muccini, F. Biscarini, and C. Taliani, Synth. Met. **101**, 592 (1999).
[10] M. Schneider, M. Brinkmann, M. Muccini, F. Biscarini, C. Taliani, W. Gebauer, M. Sokolowski, and E. Umbach, Chem. Phys. **285**, 345 (2002).
[11] E. M. Muller and J. A. Marohn, Adv. Mater. (Weinheim, Ger.) **17**, 1410 (2005).
[12] L. Burgi, T. Richards, M. Chiesa, R. H. Friend, and H. Sirringhaus, Synth. Met. **146**, 297 (2004).
[13] L. S. C. Pingree, M. C. Hersam, M. M. Kern, B. J. Scott, and T. J. Marks, Appl. Phys. Lett. **85**, 344 (2004).
[14] G. M. Credo, D. L. Winn, and S. K. Buratto, Chem. Mater. **13**, 1258 (2001).
[15] M. Muccini, Nat. Mater. **5**, 605 (2006).
[16] J. Zaumseil, R. H. Friend, and H. Sirringhaus, Nat. Mater. **5**, 69 (2006).
[17] J. S. Swensen, C. Soci, and A. J. Heeger, Appl. Phys. Lett. **87**, 253511 (2005).
[18] J. Zaumseil, C. L. Donley, J. S. Kim, R. H. Friend, and H. Sirringhaus, Adv. Mater. (Weinheim, Ger.) **18**, 2708 (2006).
[19] C. L. Donley, J. Zaumseil, J. W. Andreasen, M. M. Nielsen, H. Sirringhaus, R. H. Friend, and J. S. Kim, J. Am. Chem. Soc. **127**, 12890 (2005).
[20] M. J. Banach, R. H. Friend, and H. Sirringhaus, Macromolecules **36**, 2838 (2003).
[21] Certain equipment, instruments, or materials are identified in this paper in order to adequately specify the experimental details. Such identification does not imply recommendation by the National Institute of Standards and Technology nor does it imply the materials are necessarily the best available for the purpose.
[22] See EPAPS Document No. E-APPLAB-92-022804 for additional experimental details and results. This document can be reached through a direct link in the online article's HTML reference section or via the EPAPS homepage (http://www.aip.org/pubservs/epaps. html).
[23] H. Sirringhaus, R. J. Wilson, R. H. Friend, M. Inbasekaran, W. Wu, E. P. Woo, M. Grell, and D. D. C. Bradley, Appl. Phys. Lett. **77**, 406 (2000).
[24] Z. J. Zheng, K. H. Yim, M. S. M. Saifullah, M. E. Welland, R. H. Friend, J. S. Kim, and W. T. S. Huck, Nano Lett. **7**, 987 (2007).